Electronic Supplementary Information For:

Alternating layer addition approach to CdSe/CdS core/shell quantum dots with near-unity quantum yield and high on-time fractions

Andrew B. Greytak,*† Peter M. Allen, Jing Zhao, Wenhao Liu, Elizabeth R. Young, Zoran Popović, Brian J. Walker, Moungi G. Bawendi,* Daniel G. Nocera*

Department of Chemistry, Massachusetts Institute of Technology, 77 Massachusetts Ave., Cambridge MA 02139.

†Present address: Department of Chemistry and Biochemistry, University of South Carolina, 631 Sumter St, Columbia, SC 29208.

*Email: greytak@chem.sc.edu, nocera@mit.edu, mgb@mit.edu

Contents ***Page***

Experimental Methods

Materials: TOPO (99%), decylamine, ODE, oleic acid, and oleylamine were purchased from Aldrich. TOP, CdO, and Et_2Zn were purchased from Strem. Selenium and TMS_2S were purchased from Alfa Aesar. TOPSe (1.5 M) was prepared by dissolving Se in TOP. A stock solution of Cd oleate in ODE (0.2 M) was prepared by heating CdO in ODE with 2.1 eq. of oleic acid at 300°C under nitrogen followed by degassing under vacuum at a lower temperature. DHLA-PEG and PIL ligands were prepared as described in Refs. [S1] and [S2] respectively.

Synthesis of CdSe nanocrystal cores: Cadmium selenide nanocrystal cores were synthesized in a solvent TOP (3 ml) and TOPO (3 g). The Cd precursor was generated in situ by heating CdO with tetradecylphosphonic acid (TDPA) at 330°C under flowing nitrogen until the solution became colorless. Following removal of evolved H_2O under vacuum at reduced temperature, the solution was heated to 360°C under nitrogen. A solution of TOPSe in TOP was rapidly introduced, and the system was allowed to react at ~300°C for a short time before cooling to room temperature and storage as a yellow waxy solid. The batch used in samples **1A** and **1B** was prepared using a Se:TDPA:Cd ratio of 2.25:2:1.

CdS overcoating: A portion of the crude CdSe core batch was warmed gently, diluted with hexanes, and centrifuged to remove any undissolved material. The QDs were then flocculated by addition of acetone and/or methanol. After decanting the supernatant liquid, the QDs were brought into hexanes and held as such at 4°C for a period of 24 hours; this treatment caused precipitation of a colorless byproduct and was found to be effective in suppressing nucleation of CdS nanoparticles during subsequent shell growth. The sample was again centrifuged, and any precipitated material discarded, prior to addition of butanol and methanol to flocculate the QDs a second time. After this, the QDs were brought into a measured volume of hexane and their UV-

VIS absorption spectrum was recorded at measured dilution to gauge the size and quantity of QDs.

The QDs were introduced to a solvent of 2:1 octadecene:oleylamine (v/v, 9 mL total) and degassed at 100°C to remove hexanes. The system was placed under nitrogen and heated to 180°C before commencing reagent addition via syringe pump. Solution A (Cd precursor): to a solution of 0.2 M Cd oleate in octadecene was added 2 equivalents of decylamine, as well as a volume of TOP to yield a Cd concentration of 0.1 M. Solution B (S precursor) was a 0.1 M solution of TMS_2S in TOP. Alternating injections of Solutions A and B were performed, using Solution A (Cd) first, with injections starting every 15 minutes. The injection flow rate was adjusted so that the desired dose for each cycle was added over the course of 3 minutes. At the conclusion of the reaction, the temperature was reduced to ambient, and the sample (a strongly colored and strongly fluorescent oil) was retrieved quantitatively and its total volume recorded to aid in calculation of the molar extinction coefficient.

Elemental Analysis: Wavelength Dispersive Spectroscopy (WDS) was used to determine the elemental composition of the QD inorganic core. Dried QD samples were placed onto a silicon wafer and coated with amorphous carbon to prevent charging during measurements. Samples were then analyzed by WDS on a JEOL 733 scanning electron microscope (SEM). The results from five representative areas of the sample were averaged to obtain the data presented in Table S1.

Quantum yield measurement: Absolute quantum yields were measured using an integrating sphere that was previously described.[S3] Briefly, laser excitation (514 nm) was directed to an integrating sphere in which an NMR tube containing the sample (1 mL) was placed. Reference signals (i.e. solutions without emitting species) were also collected. Output light from the sphere was passed through a 504 nm cutoff filter and collected on a calibrated photodetector. The quantum yield value was obtained by dividing the difference of sample and reference signals (with cutoff filter) with the difference of reference and sample signals without a cutoff filter. This method was verified by measuring quantum yields of standard laser dyes: Rhodamine 101: 0.99 (ref: 1.00 [S4]), Rhodamine B: 0.33 (ref: 0.31 [S4]).

For relative quantum yield measurements, fluorescence spectra of sample and reference were recorded using a BioTeK plate reader under 450 nm excitation. Measurements were conducted in triplicate and averaged. The optical density was kept below 0.1 between 400-800 nm, and the integrated intensities of the emission spectra, corrected for differences in optical density (measured at the excitation wavelength) and the solvent index of refraction, were used to calculate the quantum yields using the expression $QY_{QD} = QY_{Dye} \times (\text{Absorbance}_{dye} / \text{Absorbance}_{QD}) \times (\text{Peak Area}_{QD} / \text{Peak Area}_{Dye}) \times (n_{QD\ solvent})^2/(n_{Dye\ solvent})^2$.

Ligand exchange with DHLA-PEG and Polymeric Imidazole Ligands (PILs): For each sample, QDs (2 nmol) were flocculated from the growth solution by addition of acetone. For the thiol ligand, QD were stirred with 50 mg of the ligand mixture in 75 μL $CHCl_3$ at 60°C for 30 min under N_2. For the PIL, QDs were stirred with 5 mg ligand in 30 μL $CHCl_3$ at room temperature for 10 minutes under air, after which 30 μL methanol was added and stirring continued for 20 additional minutes. In each case, after the elapsed time, the addition of EtOH (30 μL), $CHCl_3$ (30 μL), and excess hexanes brought about the flocculation of the QDs. The sample was centrifuged. The clear supernatant was discarded, and the pellet dried in vacuo. The sample was then brought into aqueous solution by the addition of phosphate buffered saline (500 μL, pH 7.4). Aqueous samples were dialyzed several times with additional PBS prior to measurement using centrifugal concentrator tubes.

Time-resolved PL measurements: PL decay measurements for the QDs were made using the frequency doubled (400 nm) output of a sub-picosecond chirped-pulse amplified Ti:sapphire laser system that was previously described.[S5] The detector was a Hamamatsu C4334 Streak Scope streak camera. Samples were illuminated in 2 mm pathlength cuvettes at a repetition rate of 1 kHz with vigorous stirring, and the observed changes in decay kinetics with power were reversible.

For single QD blinking experiments, CdSe(CdS) QDs were spun from a dilute toluene/polymethylmethacrylate solution onto a cover glass (Electron Microscopy Sciences). Individual QDs were observed by confocal epifluorescence microscopy through a 100x, 1.40 NA oil immersion objective (Nikon). The QDs were excited with a 200 nW, 514 nm continuous-wave beam from an Ar^+ laser, and the emission was collected using an avalanche photodiode (Perkin Elmer). To estimate the QD excitation rate, we divide the beam power by the area of a diffraction-limited spot with radius $r = 0.61\times\lambda/\mathrm{NA}$ to find an excitation power density of 130 W/cm^2. Based on the solution extinction spectra, we estimate the absorption cross section of a single QD at 514 nm to be 6×10^{-16} cm^2 and 1×10^{-15} cm^2 for samples **1A** and **2** respectively, yielding maximum excitation rates of 2×10^5 s^{-1} and 3.4×10^5 s^{-1}. The maximum counts per second in the emission traces are less than these values because of limited collection angle and optical losses.

Figure S1

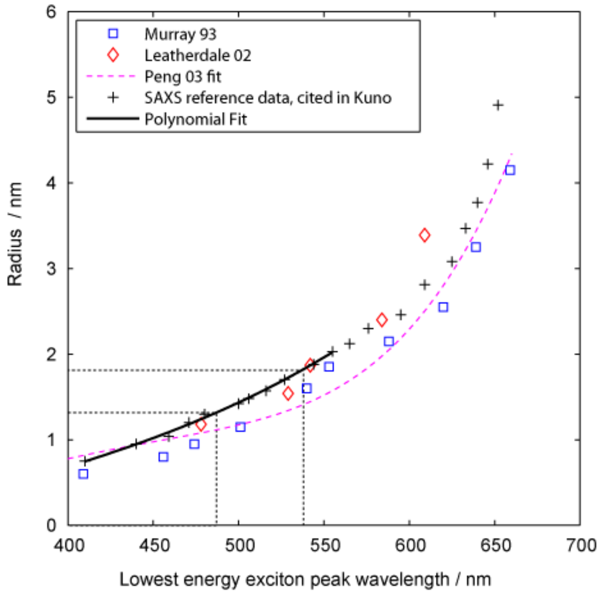

The size calibration curve shown above (solid black line) was used to assign the nominal radius of CdSe NC cores. The curve is a third-order polynomial fit of radius versus lowest energy absorption wavelength to the data points shown in black crosses over a selected range. The data and fit are reproduced from Ref. [S6] and are extracted from small angle X-ray scattering (SAXS) measurements corroborated by TEM. These are plotted alongside selected alternative size calibration data sets (Murray et al., Ref. [S7], and Leatherdale et al., Ref. [S8]). The purple curve is generated from the polynomial fit coefficients cited in Yu et al. (Ref.[S9]). The dotted black lines are guides indicating the values for the CdSe cores use to form samples **1A/1B** and **2** as described in the main text.

Figure S2

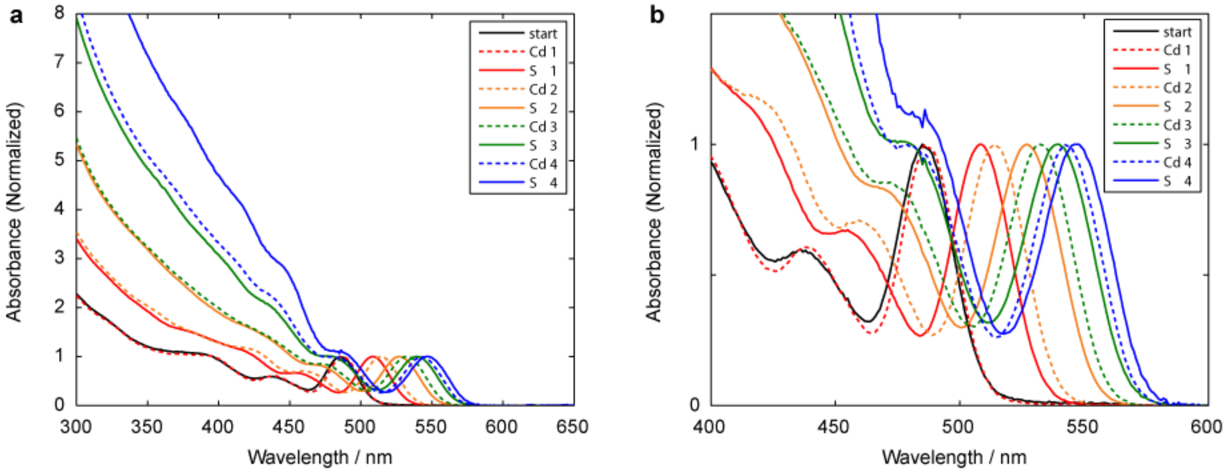

(a) Absorption spectra of aliquots taken during the synthesis of sample **1B**, normalized to 1 at the position of the lowest-energy exciton peak. Aliquots were taken prior to the start of the reaction, and then after each half-cycle of the SILAR process had been given time to react (14 minutes after the start of each 3-minute reagent addition step). **(b)** Expanded view (400-600 nm) of the spectra shown in **(a)**.

Figure S3

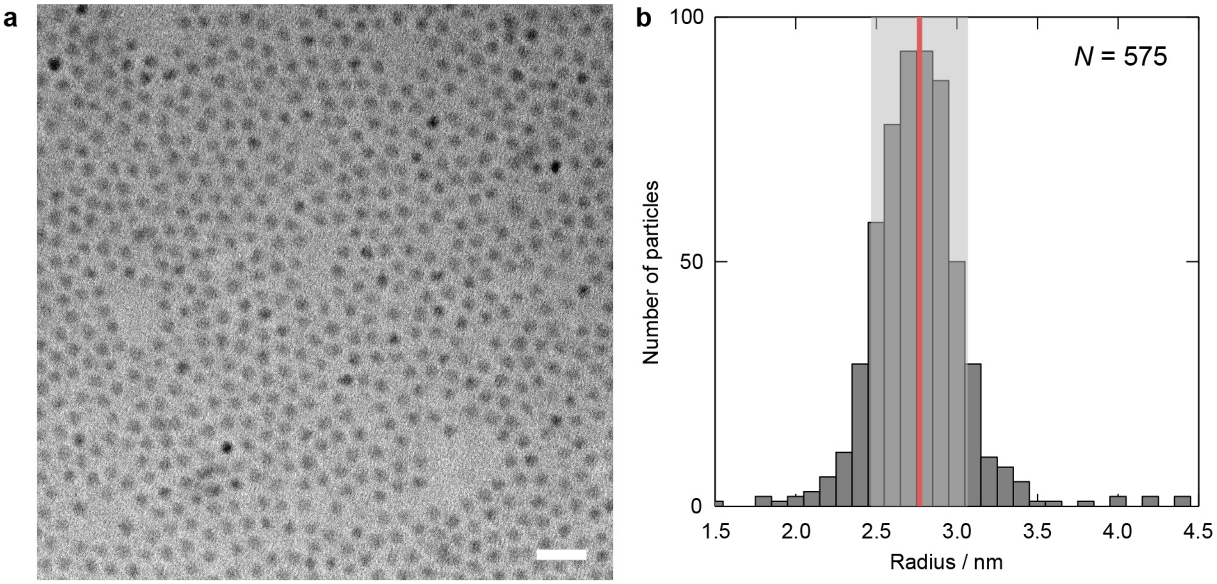

(a) A representative transmission electron microscopy (TEM) image of CdSe/CdS core/shell nanocrystals (sample **1A** from the main text). Scale bar: 20 nm. **(b),** Size distribution of particles shown in **(a)**. The red line indicates the number-average radius of 2.75 nm and the shading indicates the width of one standard deviation.

Table S1. Wavelength Dispersive Spectroscopy Results for Sample **1B** and **1B-ZnS**

	Cd	Zn	S	Se
CdSe/CdS	51.5 ± 0.7 %	0.17 ± 0.02 %	39.8 ± 0.8 %	8.4 ± 0.5 %
CdSe/CdS/ZnS	38.9 ± 0.6	11.8 ± 0.5	43.1 ± 0.7	6.1 ± 0.3

Figure S4

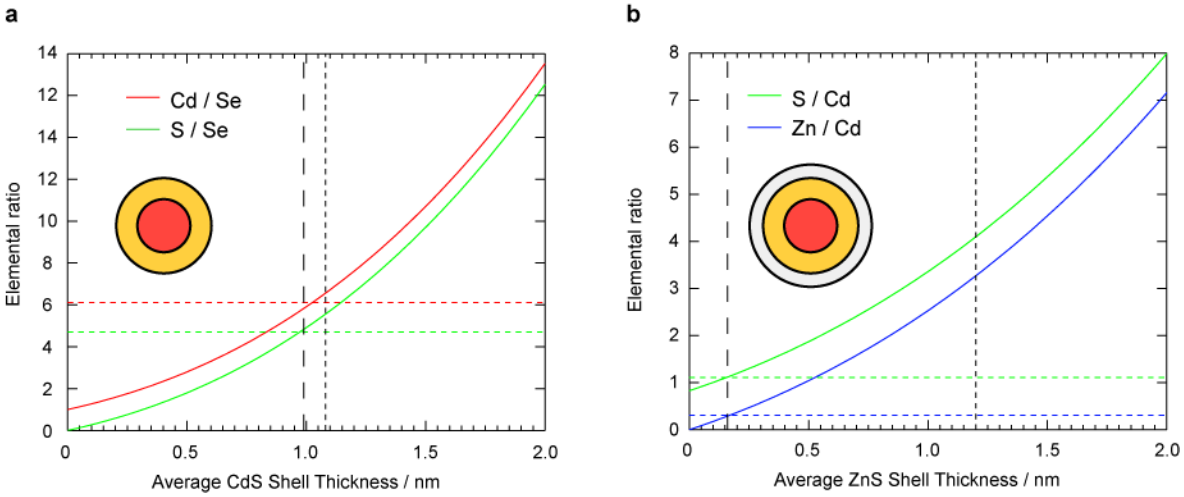

Wavelength Dispersive Spectroscopy (WDS) analysis for samples **1B** and **1B-ZnS**. **(a)** CdS shell growth on CdSe cores. Solid lines represent predicted dependence of elemental mole ratios on shell thickness, for 1.32 nm core radius spherical particles with completely relaxed strain (i.e., bulk unit cell volumes). Horizontal lines indicated experimentally observed ratios. The vertical dashed and broken lines indicate the predicted shell thickness and the thickness that is consistent with WDS data, respectively. **(b)** ZnS shell growth on CdSe/CdS core/shell particles. In this plot the WDS result for the CdS shell thickness is used to establish the radius of the particles prior to ZnS shell growth.

Figure S5

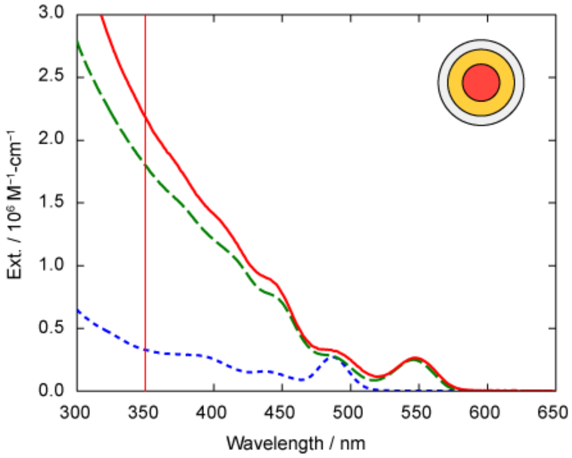

Absorption spectra of samples **1B** (dashed line), **1B-ZnS** (solid line), and the initial CdSe QD cores (dotted line) scaled to reflect calculated extinction coefficient at 350 nm.

Table 2: Representative reports of ensemble QYs for overcoated CdSe QDs

Core radius	Shell thickness	Method	Ensemble QY	Ref
	CdS shell			
1.3 nm	1.3 nm	SILAR[a]	98%	This work (**1A**)
1.2	0.7	Simultaneous[d]	50-100%[f]	Peng et al.[S10]
1.7	1.7	SILAR[b]	40%	Li et al.[S11]
1.6	1.4	SILAR[b]	65%	Xie et al.[S12]
2	6	SILAR[b]	40%	Chen et al.[S13]
2	< 6	SILAR[b]	Up to 90%	Chen et al.[S13]
2.5	4	SILAR[b]	70%	Mahler et al.[S14]
1.3	2.2	SILAR[b]	70%[c]	van Embden et al.[S15]
	ZnS or CdZnS shell			
1.5	0.6 ZnS	Simultaneous[d]	50%	Hines & Guyot-Sionnest[S16]
2.1	0.4 ZnS	Simultaneous[d]	50%	Dabbousi et al.[S17]
6	1-5[e]	Commercial (QDC)	100%	McBride et al.[S18]
1.6	1 (graded CdS/ZnS)	SILAR	80%	Xie et al.[S12]

a. TMS$_2$S sulfur precursor

b. ODE/S sulfur precursor

c. Activated with addition of trioctylphosphine and octadecylamine

d. Using Et$_2$Zn or Me$_2$Cd and TMS$_2$S

e. Highly anisotropic shell coverage

f. Relative QYs; sample-to-sample variation reported.

References

[S1] W. Liu, M. Howarth, A. B. Greytak, Y. Zheng, D. G. Nocera, A. Y. Ting, and M. G. Bawendi, *J. Am. Chem. Soc.*, 2008, **130**, 1274-1284

[S2] W. Liu, A. B. Greytak, J. Lee, C. R. Wong, J. Park, L. F. Marshall, W. Jiang, P. N. Curtin, A. Y. Ting, D. G. Nocera, D. Fukumura, R. K. Jain, and M. G. Bawendi, *Journal of the American Chemical Society*, 2010, **132**, 472-483

[S3] Z. Popović, W. Liu, V. P. Chauhan, J. Lee, C. Wong, A. B. Greytak, N. Insin, D. G. Nocera, D. Fukumura, R. K. Jain, and M. G. Bawendi, *Angewandte Chemie International Edition*, 2010, **49**, 8649-8652

[S4] D. Magde, G. E. Rojas, and P. G. Seybold, *Photochemistry and Photobiology*, 1999, **70**, 737-744

[S5] Z.-H. Loh, S. E. Miller, C. J. Chang, S. D. Carpenter, and D. G. Nocera, *The Journal of Physical Chemistry A*, 2002, **106**, 11700-11708

[S6] M. K. Kuno, PhD Thesis, MIT, 1998

[S7] C. B. Murray, D. J. Norris, and M. G. Bawendi, *Journal of the American Chemical Society*, 1993, **115**, 8706-8715

[S8] C. A. Leatherdale, W. K. Woo, F. V. Mikulec, and M. G. Bawendi, *Journal of Physical Chemistry B*, 2002, **106**, 7619-7622

[S9] W. W. Yu, L. Qu, W. Guo, and X. Peng, *Chemistry of Materials*, 2003, **15**, 2854-2860

[S10] X. Peng, M. C. Schlamp, A. V. Kadavanich, and A. P. Alivisatos, *Journal of the American Chemical Society*, 1997, **119**, 7019-7029

[S11] J. J. Li, Y. A. Wang, W. Z. Guo, J. C. Keay, T. D. Mishima, M. B. Johnson, and X. G. Peng, *J. Am. Chem. Soc.*, 2003, **125**, 12567-12575

[S12] R. Xie, U. Kolb, J. Li, T. Basche, and A. Mews, *J. Am. Chem. Soc.*, 2005, **127**, 7480-7488

[S13] Y. Chen, J. Vela, H. Htoon, J. L. Casson, D. J. Werder, D. A. Bussian, V. I. Klimov, and J. A. Hollingsworth, *J. Am. Chem. Soc.*, 2008, **130**, 5026-5027

[S14] B. Mahler, P. Spinicelli, S. Buil, X. Quelin, J.-P. Hermier, and B. Dubertret, *Nat Mater*, 2008, **7**, 659-664

[S15] J. van Embden, J. Jasieniak, and P. Mulvaney, *Journal of the American Chemical Society*, 2009, **131**, 14299-14309

[S16] M. A. Hines and P. Guyot-Sionnest, *Journal of Physical Chemistry*, 1996, **100**, 468-471

[S17] B. O. Dabbousi, J. Rodriguez-Viejo, F. V. Mikulec, J. R. Heine, H. Mattoussi, R. Ober, K. F. Jensen, and M. G. Bawendi, *The Journal of Physical Chemistry B*, 1997, **101**, 9463-9475

[S18] J. McBride, J. Treadway, L. C. Feldman, S. J. Pennycook, and S. J. Rosenthal, *Nano Letters*, 2006, **6**, 1496-1501